
HumanSplat: Generalizable Single-Image Human Gaussian Splatting with Structure Priors

Panwang Pan^{*1}, Zhuo Su^{*†1}, Chenguo Lin^{*1,2}, Zhen Fan¹, Yongjie Zhang¹, Zeming Li¹,
Tingting Shen³, Yadong Mu², Yebin Liu^{‡4}

* Equal contribution † Project lead ‡ Corresponding author

¹ByteDance, ²Peking University, ³Xiamen University, ⁴Tsinghua University

Abstract

Despite recent advancements in high-fidelity human reconstruction techniques, the requirements for densely captured images or time-consuming per-instance optimization significantly hinder their applications in broader scenarios. To tackle these issues, we present **HumanSplat** that predicts the 3D Gaussian Splatting properties of any human from a single input image in a generalizable manner. In particular, HumanSplat comprises a 2D multi-view diffusion model and a latent reconstruction transformer with human structure priors that adeptly integrate geometric priors and semantic features within a unified framework. A hierarchical loss that incorporates human semantic information is further designed to achieve high-fidelity texture modeling and better constrain the estimated multiple views. Comprehensive experiments on standard benchmarks and in-the-wild images demonstrate that HumanSplat surpasses existing state-of-the-art methods in achieving photorealistic novel-view synthesis. Project page: <https://humansplat.github.io/>

1 Introduction

Realistic 3D human reconstruction is a fundamental task in computer vision with widespread applications in numerous fields, including social media, gaming, e-commerce, telepresence, etc. Previous works for single-image human reconstruction can be broadly categorized into explicit and implicit approaches. Explicit methods [1–4], such as those based on parametric body models like SMPL [5, 6], estimate human meshes by directly optimizing parameters and clothing offset to fit the observed image. However, these methods often struggle with complex clothing styles and require lengthy optimization. Implicit methods [7–11] represent humans using continuous functions, such as occupancy [7], SDF [12], and NeRF [13]. They are good at modeling flexible topology but are limited in scalability and efficiency due to the high computational cost of training and inference. Recent advances in 3D Gaussian Splatting [14] (3DGS) have provided a balance between efficiency and rendering quality for reconstructing detailed 3D human models, which however rely on multi-view [15–17] or monocular video [18–20] inputs. Recent popular human reconstruction studies [21–24] focus on the score distillation sampling (SDS) technique [25] to lift 2D diffusion priors to 3D, but time-consuming optimization (e.g., 2 hours) is required for each instance. Some generalizable and large-reconstruction-model-based works [10, 26–28] can directly generalize the regression of 3D representations but either disregard human priors or require multi-view inputs, limiting the stability and feasibility in downstream applications.

In this paper, we propose a novel generalizable approach **HumanSplat** for single-image human reconstruction by introducing a generalizable Gaussian Splatting framework with a pre-trained 2D video diffusion model and well-designed 3D human structure priors. Different from the existing human 3DGS methods, our approach directly infers Gaussian properties from a single image, obviating the

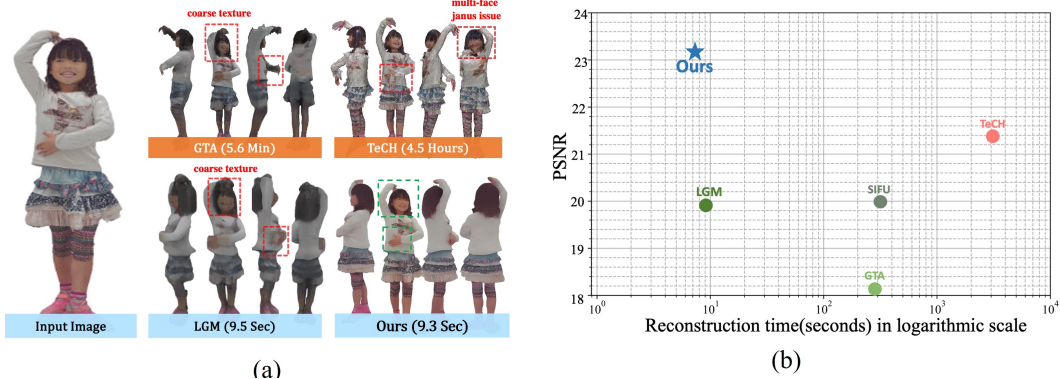


Figure 1: Our method achieves state-of-the-art rendering quality while maintaining the fastest runtime. (a) Qualitative results: LGM [29] and GTA [30] are generalizable but in lower quality, TeCH [21] exhibits issues with multi-face rendering and is time-consuming. In contrast, our method achieves higher fidelity in a much shorter time. (b) Performance and runtime comparison: metrics are evaluated on the challenging Twindom dataset.

necessity for per-instance optimization or densely captured images and empowering to generalize effectively across diverse scenes while efficiently delivering high-quality reconstructions.

The key insight behind our method is to reconstruct Gaussian properties from the diffusion latent space in a generalizable end-to-end architecture, integrating a 2D generative diffusion model as appearance prior and a human parametric model as structure prior. Specifically, facing this under-constraint reconstruction problem from single-view input with extensive invisible regions, we first leverage a 2D video diffusion model (denoted as **novel-view synthesizer**) to hallucinate the unseen parts of clothed humans. Then a generalizable **latent reconstruction transformer** is proposed to enable interaction among the generated diffusion latent embeddings and the geometric information of the structured human model, enhancing the quality of 3DGS reconstruction. During interactions using inaccurate human prior like the SMPL model, a projection strategy is designed to balance the robustness and flexibility, where we compensate for inaccuracies by projecting 3D tokens into 2D space and conducting searches within adjacent windows using project-aware attention. Another specific challenge of human reconstruction is to capture fine detail in visually sensitive areas, such as the face and hand. To address this problem, we exploit the semantic cues from the structure priors and propose **semantics-guided objectives** to further promote the fine details reconstruction quality. By amalgamating these crucial components into a unified framework, our method achieves state-of-the-art performance in striking the right balance between quality and efficiency.

In summary, the main contributions of our work are as follows:

- We propose a novel generalizable human Gaussian Splatting network for high-fidelity human reconstruction from a single image. To the best of our knowledge, it is the first to leverage latent Gaussian reconstruction with a 2D generative diffusion model in an end-to-end framework for efficient and accurate single-image human reconstruction.
- We integrate structure and appearance cues within a universal transformer framework by leveraging human geometry priors from the SMPL model and human appearance priors from the 2D generative diffusion model. Geometric priors stabilize the generation of high-quality human geometry, while appearance prior helps hallucinate unseen parts of clothed humans.
- We enhance the fidelity of reconstructed human models by introducing semantic cues, hierarchical supervision, and tailored loss functions. Extensive experiments demonstrate that our method achieves state-of-the-art performance, surpassing existing methods.

2 Related Work

Single-Image Human Reconstruction. Single-image human reconstruction methods fall into explicit and implicit approaches. Explicit methods use parametric body models [5, 6] to estimate

minimally clothed human meshes [1, 2, 31–37], adding clothing via 3D offsets [3, 4, 38–41] or garment templates [42–44]. However, these methods are constrained by topology, particularly with loose clothing. Implicit methods [7–11, 27, 45–47], utilizing representations like occupancy, signed distance fields (SDF) and Neural Radiance Fields (NeRF), offer flexibility with topology, allowing for accurate depiction of 3D clothed humans. Recent methods [48–63] combine implicit representation with explicit human priors for better robustness. Among these, GTA [58] uses transformers with fixed embeddings for translating image features into 3D tri-plane features. TeCH [64] employs diffusion-based models for visualizing unseen areas but needs extensive optimization and accurate SMPL-X models. Another approach, HumanSGD [46], uses diffusion models for texture inpainting but struggles with mesh inaccuracies from [8]. NeRF-based methods like SHERF [10] generate human NeRFs from single images using hierarchical features, while ELICIT [11] leverages CLIP [65] for contextual understanding. These NeRF-based methods produce high-quality images but often struggle with detailed 3D mesh generation and require extensive optimization time.

Human Gaussian Splatting. While implicit representations like SDF or NeRF struggle with balance optimization efficiency and rendering quality, the high efficiency of 3DGS [66] has advanced 3D human creation. Recent 3DGS methods have targeted multi-view videos, monocular video sequences, and sparse-view input. Multi-view video methods like D3GA [15], HuGS [16], and 3DGS-Avatar [17] exploit dense spatial and temporal information for detailed models. Additionally, HiFi4G [67] combine 3DGS with a dual-graph mechanism to preserve spatial-temporal consistency, ASH [68] utilizes mesh UV parameterization for real-time rendering, and Animatable Gaussians [69] improve garment dynamics via pose projection mechanism and 2D CNNs. The monocular video only provides sufficient observation as humans move, so the monocular human Gaussian Splatting methods [18–20, 70–75] often resort to using LBS for mapping to a canonical space and introducing additional regularization terms. For sparse-view images, GPS-Gaussian [28] achieves high rendering speeds without per-subject optimization by using a feed-forward way with efficient 2D CNNs encoding from diverse 3D human scan data. In comparison, our work stands out as the first one-shot generalizable human GS method, using only single image input and achieving high-quality reconstruction without any optimization and fine-tuning.

Generalizable Large Reconstruction Model. Large reconstruction model (LRM) [76, 77] presents that with sufficient parameters and training datasets, a deterministic feed-forward Transformer [78] is capable of learning a triplane feature for volumetric rendering from a single-view image. Targeting general 3D object, TriplaneGaussian [79] combines 3DGS with triplane as a hybrid 3D representation for fast rendering, where point clouds are first extracted from an image and then projected on triplane features to decode 3DGS attributes. Most recent methods further leverage 2D diffusion models that can generate multi-view images simultaneously [80–83] to provide plausible and abundant inputs for the following reconstruction, so they focus on the sparse multi-view reconstruction task. Instant3D [83] follows the technique of LRM and produces triplane features from 4 posed images by a Transformer encoder. CRM [84], MeshLRM [85] and InstantMesh [86] replaces triplane NeRF by FlexiCubes [87] to extract meshes directly. LGM [88], GRM [89] and GS-LRM [90] predict 3DGS attributes from each input pixel [91, 92] and combine the Gaussians from multiple viewpoints as the final 3D output. For human task, CharacterGen [93] follows Instant3D [83] to adopt a two-stage approach: first, generating a 2D multi-view canonical images, then using multi-view SDF reconstruction for cartoon digital characters, without direct interaction between stages. A more compact and elegant method HumanLRM [27] replaces training data of LRM [76] from general objects with human data to predict triplane NeRF, showcasing the capacities of the large model. While it relies heavily on the dataset, often leading to issues like missing limbs due to a lack of prior knowledge. In contrast, our 3DGS-based method leverages the latent diffusion and reconstruction model in an end-to-end framework and introduces human priors by addressing their inaccuracy with specific projection strategies, achieving better generalization and stability with even less data.

3 Method

3.1 Preliminary

SMPL [5] is a widely-used parametric human body model that is created by skinning and blend shapes, and learned from thousands of 3D body scans. The SMPL model [5] utilizes shape parameters $\beta \in \mathbb{R}^{10}$ and pose parameters $\theta \in \mathbb{R}^{24 \times 3}$ to parameterize the deformation of the human body mesh $\mathcal{M}(\beta, \theta) : \beta \times \theta \mapsto \mathbb{R}^{6890 \times 3}$.

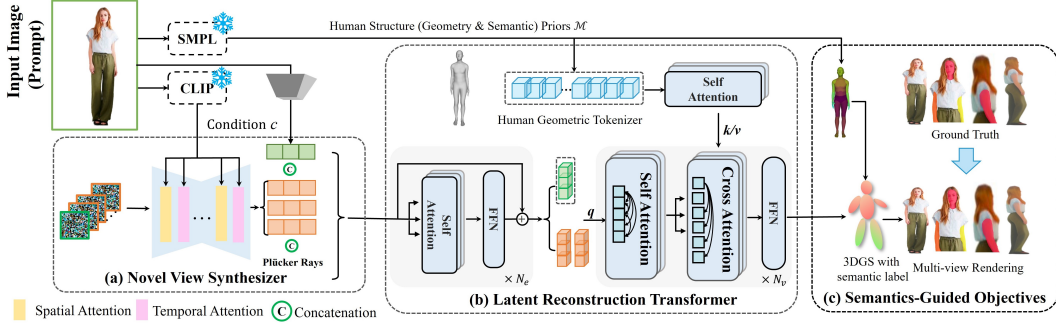


Figure 2: Overview of HumanSplat. (a) Multi-view latent features are first generated by a fine-tuned video diffusion model (Novel View Synthesizer in Sec. 3.3). (b) Then, the Latent Reconstruction Transformer (Sec. 3.4) interacts global latent features (Sec. 3.4.1) and human geometric prior (Sec. 3.4.2). (c) Finally, the semantic-guided objectives (Sec. 3.5) are proposed to reconstruct the final human 3DGS.

3D Gaussians Splatting [14] is an recently proposed 3D representation that represents 3D content by a set of N_p colored Gaussians $\mathcal{G} = \{\mathbf{g}_i\}_{i=1}^{N_p}$. Each Gaussian $\mathbf{g}_i = \exp(-\frac{1}{2}(\mathbf{x} - \boldsymbol{\mu}_i)^\top \boldsymbol{\Sigma}_i^{-1}(\mathbf{x} - \boldsymbol{\mu}_i))$ has opacity $\sigma_i \in \mathbb{R}$ and color $\mathbf{c}_i \in \mathbb{R}^3$ attributes, where $\boldsymbol{\mu}_i \in \mathbb{R}^3$ is its location and $\boldsymbol{\Sigma}_i \in \mathbb{R}^{3 \times 3}$ implies its scaling $\mathbf{s} \in \mathbb{R}^3$ and orientation quaternion $\mathbf{q} \in \mathbb{R}^4$ in 3D space. These attributes together $\mathbf{G} \in \mathbb{R}^{N_p \times 14}$ can represent a 3D object, and by projecting to the image plane with opacity-based color composition in the depth order, it can be differentially rendered into 2D images in real-time.

3.2 Overview

Given a single input image of a human body $\mathbf{I}_0 \in \mathbb{R}^{H \times W \times 3}$, our task is to reconstruct a 3D representation, i.e., 3DGS in this work, from which novel-view images can be rendered. As illustrated in Fig. 2, our method leverages a 2D diffusion model and a novel latent reconstruction transformer that adeptly integrates 2D appearance priors, human geometric priors, and semantic cues within a universal framework. First, we use SMPL estimator [94, 95] to predict human structure priors \mathcal{M} , and CLIP [65] to generate the image embedding of the input image \mathbf{c} . A latent temporal-spatial diffusion model [96], referred to as the **novel-view synthesizer** (Sec. 3.3), is fine-tuned and produces multi-view latent features $\{\mathbf{F}_i \in \mathbb{R}^{h \times w \times c}\}_{i=1}^N$, where N is the number of views, and h , w and c are the height, width and channel of the latent features. Then, we utilize a novel **latent reconstruction transformer** (Sec. 3.4) that adeptly integrates human geometric prior and latent features within a universal framework, which predicts Gaussian attributes $\mathbf{G} := \{(\boldsymbol{\mu}_i, \mathbf{q}_i, \mathbf{s}_i, \mathbf{c}_i, \sigma_i) | i = 1, \dots, N_p\}$ and rendered into new images, where N_p represents the number of Gaussian points. Furthermore, to achieve high-fidelity texture modeling and better constrain the estimated multiple views, we designed a hierarchical loss that incorporates human semantic priors (See 3.5). Note that during training, the network is trained using 3D scan data to ensure accurate supervision from various viewpoints, where the registered SMPL is fitted via the multi-view version of SMPLify [95]. During inference, the model employs PIXIE [94] to predict human structure priors \mathcal{M} and synthesize novel views from only the single image input based on the trained model, without any fine-tuning and optimization.

3.3 Video Diffusion Model as Novel-view Synthesizer

We take advantage of the pre-trained video diffusion model SV3D [96] as appearance prior. It utilizes the CLIP [65] image embedding \mathbf{c} and latent feature \mathbf{F}_0 of a input image \mathbf{I}_0 from a pre-trained VQ-VAE [97] \mathcal{E} as conditions and progressively denoises gaussian noises into temporal-continuous N multi-view latent features $\{\mathbf{F}_i\}_{i=1}^N$ by a spatial-temporal UNet D_θ [98] with the objective:

$$\mathbb{E}_{\epsilon \sim p(\epsilon)} [\lambda(\epsilon) \|D_\theta(\{\mathbf{F}_i^\epsilon\}_{i=1}^N; \mathbf{c}, \mathbf{F}_0, \epsilon) - \{\mathbf{F}_i\}_{i=1}^N\|_2^2], \quad (1)$$

where $\{\mathbf{F}_i^\epsilon\}$ is the noise-corrupt multi-view latent features, $p(\epsilon)$ is the noise probability distribution and $\lambda(\epsilon) \in \mathbb{R}^+$ is the loss weighting term related to the noise level ϵ . Since SV3D is merely pre-trained on the dataset of objects [99], we further fine-tune it using human datasets to improve its effectiveness in the human reconstruction task. More technical details are available in Appendix A.1.

3.4 Latent Reconstruction Transformer

Latent reconstruction transformer contains two parts: **latent embedding interaction** (Sec. 3.4.1) and **geometry-aware interaction** (Sec. 3.4.2), which seamlessly incorporate latent features from video diffusion and human structure priors into the reconstruction process. The two components together form a cohesive framework for accurately recovering intricate human details.

3.4.1 Latent Embedding Interaction

We utilize a pretrained VQ-VAE [97] \mathcal{E} to encode the input image \mathbf{I}_0 into a latent representation $\mathbf{F}_0 = \mathcal{E}(\mathbf{I}_0) \in \mathbb{R}^{h \times w \times c}$ and combine it with the generated $\{\mathbf{F}_i\}_{i=1}^N$ (Sec. 3.3). Following previous works [100, 101], Plücker ray embeddings [102] are leveraged for pose conditioning, where latent representations are concatenated with their corresponding Plücker coordinates along the channel dimension, resulting in a per-pixel pose-conditioned feature map. These latents are then divided into non-overlapping patches [103] and mapped to d -dimensional latent tokens by a linear layer. An intra-attention module is followed to thoroughly extract spatial correlations of latent tokens, as shown in Fig. 3. The intra-attention module is implemented using a standard Transformer [78] with multiple blocks of multi-head self-attention and feed-forward network (FFN):

$$\bar{\mathbf{F}}_0, \bar{\mathbf{F}}_1, \dots, \bar{\mathbf{F}}_N = \text{FFN}(\text{SelfAttention}(\mathbf{F}_0, \mathbf{F}_1, \dots, \mathbf{F}_N)). \quad (2)$$

3.4.2 Geometry-aware Interaction

Human Geometric Tokenizer. Given a human geometric model $\mathcal{M} \in \mathbb{R}^{6890 \times 3}$, to obtain the feature representation at a position $x \in \mathbb{R}^3$, we project x onto input view and computes the feature vector through bilinear interpolation on the feature grids by

$$\mathbf{\Pi}_i(x) = \mathbf{K}(\mathbf{R}\mathcal{M}_i + \mathbf{t}), \quad (3)$$

where \mathbf{R}, \mathbf{t} are camera extrinsic parameters, \mathbf{K} is the intrinsic parameters. After the projection operation, we obtain geometric human prior tokens by concatenating x and $\mathbf{F}_0(\mathbf{\Pi}(x))$, and mapping them to d dimension. Similar to Latent Embedding Interaction, an intra-attention module is utilized to interact among these human prior tokens and get geometric features $\bar{\mathbf{H}}_i \in \mathbb{R}^{6890 \times d}$.

Human Geometry-aware Attention. Empirically, we find that incorporating human priors [5, 6, 104] (e.g., SMPL model) into human reconstruction faces a significant dilemma of the trade-off between robustness and flexibility [30, 105]. On the one hand, the SMPL model provides geometric priors that alleviate common issues (e.g., broken body parts and various artifacts). On the other hand, it struggles to accurately capture and represent a broad spectrum of complex clothing styles, particularly more fluid garments like dresses and skirts. This limitation highlights a fundamental shortcoming in the model’s capacity to accurately depict diverse apparel. As shown in Fig. 3, HumanSplat efficiently utilizes priors while accounting for their inaccuracies by projecting 3D tokens into 2D space and searching in the nearby windows. To tackle the issue of matching redundancy with erroneous human priors, HumanSplat leverages these priors while compensating for their inaccuracies by projecting 3D tokens into 2D space and conducting searches within adjacent windows. Specifically, we introduce project-aware attention within the inter-attention module, utilizing a window $\mathbf{W}(k_{win} \times k_{win})$ and employing masked multi-head cross-attention. Here, the latent features $\{\bar{\mathbf{F}}_i\}$ serve as queries, and the human prior tokens $\{\bar{\mathbf{H}}_i\}$ serve as keys/values. The process can be formulated as follows:

$$\tilde{\mathbf{F}}_i = \text{FFN}(\text{CrossAttention}_{mask}(\bar{\mathbf{F}}_i, \bar{\mathbf{H}}_i)), \quad (4)$$

where feature interactions occur when $\mathbf{\Pi}(\bar{\mathbf{H}}_i, \mathbf{K}, \mathbf{R}, \mathbf{t})$ is within the window of $\bar{\mathbf{F}}_i$. It is noteworthy that the complexity of the cross-attention operation is reduced from $\mathcal{O}(\mathbf{L}_F \times \mathbf{L}_H)$ to $\mathcal{O}(\mathbf{L}_F \times k_{win}^2)$, compared to the vanilla multi-head Cross-attention setting. Here, \mathbf{L}_F and \mathbf{L}_H represent the lengths of the latent and human prior tokens respectively.

3.5 Semantics-guided Objectives

From each output token $\tilde{\mathbf{F}}_i$, we decode the attributes of pixel-aligned Gaussians \mathbf{G} in the corresponding patch by a convolutional layer with a 1×1 kernel. These attributes are used to render novel view images through 3D Gaussian Splatting. An ideal training objective should ensure that the

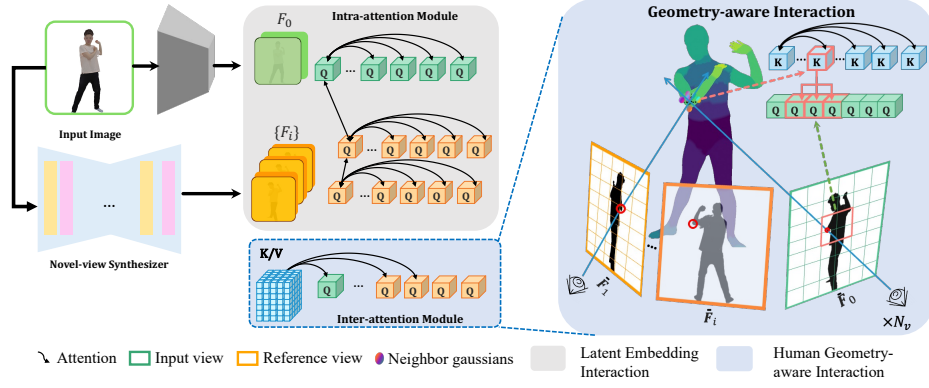


Figure 3: Illustration of latent reconstruction transformer. It first divides F_0 and F_i into non-overlapping patches, which are then processed through an intra-attention module (Sec. 3.4.1). Within the inter-attention module (Sec. 3.4.2), we introduce the project-aware attention with a window $W(k_{win} \times k_{win})$, and the attributes of 3D Gaussians are decoded with a Conv 1×1 layer.

rendered outputs closely match the supervised images, striving for overall consistency between the reconstructed renderings and the ground truth. However, human attention tends to be particularly focused on facial regions, where intricate details play a pivotal role in perception. Therefore, in our quest to elevate the fidelity of reconstructed human models, we introduce a paradigm shift in our training objectives.

Hierarchical Loss. Traditional approaches often overlook the semantic richness inherent in human anatomy, leading to reconstructions that lack crucial details and accuracy. To address this, we propose a novel framework that harnesses semantic cues, hierarchical supervision, and tailored loss functions to guide the training process. This ensures that not only are the overall structures of the human body accurately represented, but also that critical areas such as the face are reconstructed with exceptional detail and fidelity. Specifically, by incorporating a human prior model equipped with semantic information, we establish direct correspondences between 3D spatial positions and specific human body parts. Therefore, we can utilize different attention weights for different body parts and render different levels of GT images from different viewpoints to provide hierarchical supervision. This approach significantly facilitates the precise localization of essential body parts, including the head, hands, and arms. The overall loss is defined as a weighted sum of part-specific losses:

$$\mathcal{L}_{\mathcal{H}} = \frac{1}{l} \frac{1}{n} \sum_{i=1}^n \sum_{j=1}^m \lambda_i \lambda_j \mathcal{L}_{Rec}(\mathbf{I}_{part,j}, \hat{\mathbf{I}}_{part,j}), \quad (5)$$

where $i \in \{1, \dots, n\}$ and $j \in \{1, \dots, m\}$ denote different resolution levels and human parts. $\hat{\mathbf{I}}_{part,j}$ and $\mathbf{I}_{part,j}$ are the predicted and ground-truth data for part j , λ_i and λ_j are weighting factors that reflect the relative importance of each resolution level and each body part, respectively.

Reconstruction Loss. Reconstruction loss L_{Rec} based on the N_{render} rendered multi-view images is defined as

$$\mathcal{L}_{Rec} = \sum_i^{N_{render}} \mathcal{L}_{mse}(\hat{\mathbf{I}}_i, \mathbf{I}_i) + \lambda_m \mathcal{L}_{mse}(\hat{\mathbf{M}}_i, \mathbf{M}) + \lambda_p \mathcal{L}_p(\hat{\mathbf{I}}_i, \mathbf{I}_i), \quad (6)$$

where \mathbf{I}_i and $\hat{\mathbf{I}}_i$ are the ground-truth images and render images via Gaussian Splatting, \mathbf{M}_i and $\hat{\mathbf{M}}_i$ are original and rendered foreground mask. \mathcal{L}_{mse} measures the MSE loss and \mathcal{L}_p measures the perceptual loss [106]. λ_m and λ_p are hyperparameters for balancing. The final training objective is a combination of the two loss terms: $\mathcal{L} = \mathcal{L}_{\mathcal{H}} + \mathcal{L}_{Rec}$.

4 Experiments

4.1 Implementation Details

Training Details. HumanSplat is trained on 500 THuman2.0 [107], 1500 2K2K [108], and 1500 Twindom [109] high-fidelity human scans. We evenly position 36 cameras across each of three hierarchical cycles to capture the full body, half body, and face, with rendering resolution set to 512×512 . We conduct 200 epochs of training with a learning rate of $1e-5$ and a batch size of 32 over 4 days, utilizing 8 NVIDIA A100 GPUs. Additional implementation details are provided in Appendix A.3.

Inference time. The 2D Video Diffusion model takes about 9s to generate multi-view latent features while the subsequent latent reconstruction for 3DGS takes only 0.3s. Additionally, it can render novel views at a rate exceeding 150 FPS on a single NVIDIA A100 GPU.

4.2 Comparison

Baselines. We evaluate novel view synthesis using state-of-the-art methods such as GTA [30] and SIFU [105] by rendering textured meshes from multiple angles and calculating the PSNR to ground truth images. We divided 21 scans from Thuman2.0 [107] and 51 scans from Twindom [109] for evaluation. To eliminate the bias of the training dataset, we fine-tune the generative model LGM [29] on the same datasets as ours for a fair comparison. Additionally, we optimized each instance of TeCH [21] until full convergence for comparison.

Quantitative Comparison. Following baseline methods [21, 22, 105], we utilize PSNR, SSIM [110] and VGG-LPIPS [106] as evaluation metric. As shown in Tab. 1, HumanSplat consistently outperforms previous generalizable methods across all datasets. Specifically, HumanSplat surpasses SIFU [105] by +1.92 (8.72%) in PSNR and reduces LPIPS from 0.079 to 0.055. Notably, HumanSplat also excels on the more challenging Twindom dataset, outperforming TeCH[21] by +2.15 (10.16%) in PSNR and reducing LPIPS from 0.188 to 0.125. Although the values can further decrease with model training, we control the convergence to the current extent in the dataset for better generalization under more general in-the-wild scenarios. Besides, we also report the reconstruction times for 512×512 input images on identical NVIDIA A100 hardware. HumanSplat achieves remarkably fast reconstruction times, approximately 9.3 seconds, on a single NVIDIA A100 GPU, making it highly practical compared to TeCH’s 4.5-hour reconstruction time.

Qualitative Comparison. By incorporating semantics-guided objectives, Humansplat achieves more detailed and higher fidelity results against GTA [30] and LGM [29], as illustrated in Fig. 4. Results on in-the-wild images demonstrate our strong generalization capability. Although TeCH [21] also generates high quality image, its SDS optimization often results in overly saturated multi-face outcomes [111, 112]. Moreover, while TeCH delivers highest PSNR on the Thuman2.0 dataset, the LPIPS metric in Tab. 1, confirms that our method delivers more realistic results. Notably, our model provides superior textures on both the front and invisible regions, highlighting the effectiveness of incorporating appearance and geometric priors.

4.3 Ablation Study

Latent Reconstruction Transformer. HumanSplat leverages the Stable Diffusion latent space for feature extraction. Experimental results demonstrate that utilizing the compact latent space for reconstructions leads to better rendering quality compared to using the pixel space, as detailed in Tab. 2 (a). We also find that patching in the time dimension for latent decoding by temporal VAE [98] adversely affects the quality, so we employ the vanilla VQ-VAE [97] decoder in this work.

Human Geometric Prior. To evaluate the robustness of HumanSplat to SMPL parameters, we employed various initialization strategies for the geometry. The results of these different methods are presented in Table 2 (b). In cases where the SMPL initialization involved extreme randomness, our model demonstrated robustness against SMPL estimation errors, as our approach of treating human priors as keys and values. Furthermore, the projection window k_{win} ensures that parameters estimated from a single view detector [2], as well as results from the multi-view version of SMPLify [95], remain within acceptable tolerances. The effectiveness of the human geometric prior is also demonstrated qualitatively in Figure 5 (a).

Table 1: Quantitative comparison on texture against other methods. * indicates that this method is fine-tuned on our training dataset. † indicates that this method requires per-instance optimization.

Method	Category		THuman2.0 [107]			Twindom [109]			Rec. Time
	Diffusion	Human Prior	PSNR↑	SSIM↑	LPIPS↓	PSNR↑	SSIM↑	LPIPS↓	
PIFu [113]	✗	✗	18.093	0.911	0.137	-	-	-	~30 Sec
LGM* [29]	✓	✗	20.013	0.893	0.116	19.840	0.851	0.292	~9.5 Sec
GTA [30]	✗	✓	18.050	-	-	17.669	0.741	0.418	~5.6 Min
SIFU [105]	✗	✓	22.025	0.921	0.084	19.714	0.832	0.312	~5.7 Min
SIFU† [105]	✓	✓	22.102	0.923	0.079	-	-	-	~5.7 Min
Magic123† [114]	✓	✗	14.501	0.874	0.145	-	-	-	~1 Hours
HumanSGD† [22]	✓	✓	17.365	0.895	0.130	-	-	-	~7 Min
TeCH† [21]	✓	✓	25.211	0.936	0.083	<u>21.192</u>	<u>0.884</u>	<u>0.188</u>	~4.5 Hours
HumanSplat (Ours)	✓	✓	<u>24.033</u>	<u>0.918</u>	0.055	23.346	0.913	0.125	~9.3 Sec



Figure 4: Qualitative comparison of ours against TeCH [21], GTA [30] and LGM [29] on Thuman2.0 [107], Twindom [109] and in-the-wild images. Our method achieves the highest quality. Note that TeCH achieves clearer results but fails to preserve the face ID.

Table 2: Ablation study of several proposed designs on 2K2K [108] dataset.
 (a) Reconstruction Space. (b) Geometric Prior Initialization. (c) Different project methods.

Space	PSNR↑ SSIM↑ LPIPS↓	Method	PSNR↑ SSIM↑ LPIPS↓	Method	PSNR↑ SSIM↑ LPIPS↓
Pixel Space	23.125 0.892 0.066	Random	19.894 0.876 0.366	w/o Human Prior	22.635 0.893 0.182
Temporal VAE [98]	24.133 0.902 0.047	Multi-view	24.633 0.935 0.025	Project Only	23.333 0.916 0.057
Ours [115]	24.293 0.915 0.040	Ours [2]	24.293 0.915 0.040	Ours ($K_{win} = 2$)	24.293 0.915 0.040

Window Size. As analyzed in Sec. 3.4.2, human priors are crucial for the robustness of the human reconstruction model. As demonstrated in Tab. 2 (c), the PSNR metric is significantly improved from 22.625db to 24.293db. When the window size K_{win} is set to 1 (Project Only), the model struggles to handle loose clothing. We also explore how the performance of the model varies with different window sizes by setting $K_{win} = 2$, in a latent space with a resolution of 64×64 .

Semantics-guided Training Objectives. Thanks to the incorporation of semantic-guided hierarchical loss, HumanSplat can generate textures of higher quality for both the face and hand, while also promote the convergence of the training process, as depicted in Figure 5 (a) and (b). Furthermore, Figure 5 (c) demonstrates that HumanSplat further produces 3D consistent segmentation results, which have potential applications in areas such as editing and specific generation of individual parts of 3D humans.

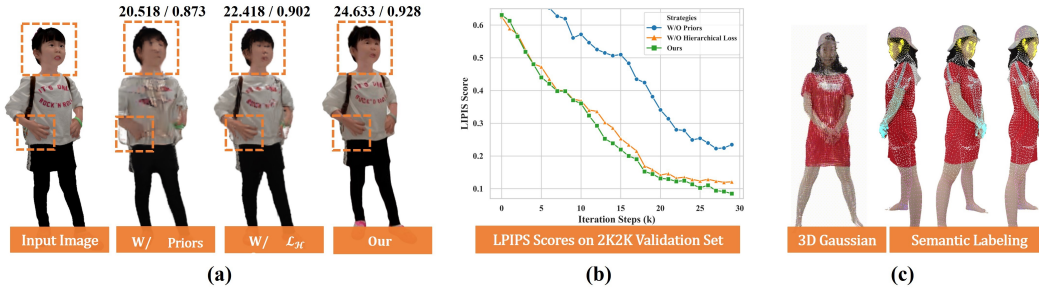


Figure 5: (a) Qualitative evaluation of human prior and hierarchical loss \mathcal{L}_H . PSNR/SSIM values are shown at the top of each image, presenting the effectiveness of the two strategies in the full pipeline. (b) LPIPS scores during training on the 2K2K validation set. (c) HumanSplat can provide 3D consistent segmentation results for potential applications.

5 Conclusion

We present HumanSplat, a pioneering generalizable Human Gaussian Splatting network that derives 3D Gaussian Splatting properties from a single image. This model integrates generative diffusion and latent reconstruction transformer models with human structure priors, enhanced by a tailored semantic-aware hierarchical loss. These innovations achieve realistic and detailed reconstructions in a fast feed-forward manner without any optimization or fine-tuning, especially in the important focal areas such as the face and hands. Extensive experiments demonstrate that HumanSplat surpasses existing state-of-the-art methods in both quality and efficiency, including robust performance in handling challenging poses and loose clothing. This capability opens up a broad spectrum of potential applications.

Limitations and Future Works. Our methods have some limitations that can be addressed in future works: (a). While effective with most attire, the model may struggle with intricate garments and accessories. Future enhancements should incorporate 2D data and innovative training strategies, which is a promising direction for improving the handling of diverse and unusual clothing styles. (b). Although already efficient, increasing the computational speed by constraining Gaussian’s number or combining compact 3DGS with texture representation could further facilitate real-time applications, particularly on mobile devices. (c). Animating the reconstructed human models currently requires post-processing. Future work could introduce canonical space to reconstruct animatable avatars directly, streamlining the process and improving efficiency.

References

- [1] Hongwen Zhang, Yating Tian, Xinchu Zhou, Wanli Ouyang, Yebin Liu, Limin Wang, and Zhenan Sun. PyMAF: 3D Human Pose and Shape Regression with Pyramidal Mesh Alignment Feedback Loop. In *ICCV*, 2021.
- [2] Yao Feng, Vasileios Choutas, Timo Bolkart, Dimitrios Tzionas, and Michael J Black. Collaborative regression of expressive bodies using moderation. In *2021 International Conference on 3D Vision (3DV)*, pages 792–804. IEEE, 2021.
- [3] Thiemo Alldieck, Gerard Pons-Moll, Christian Theobalt, and Marcus Magnor. Tex2Shape: Detailed Full Human Body Geometry From a Single Image. In *ICCV*, 2019.
- [4] Thiemo Alldieck, Marcus A. Magnor, Weipeng Xu, Christian Theobalt, and Gerard Pons-Moll. Detailed human avatars from monocular video. In *International Conference on 3D Vision (3DV)*, 2018.
- [5] Matthew Loper, Naureen Mahmood, Javier Romero, Gerard Pons-Moll, and Michael J Black. Smpl: A skinned multi-person linear model. *ACM transactions on graphics (TOG)*, 34(6):1–16, 2015.
- [6] Georgios Pavlakos, Vasileios Choutas, Nima Ghorbani, Timo Bolkart, Ahmed A. A. Osman, Dimitrios Tzionas, and Michael J. Black. Expressive body capture: 3D hands, face, and body from a single image. In *Proceedings IEEE Conf. on Computer Vision and Pattern Recognition (CVPR)*, pages 10975–10985, 2019.
- [7] Shunsuke Saito, Zeng Huang, Ryota Natsume, Shigeo Morishima, Hao Li, and Angjoo Kanazawa. PIFu: Pixel-aligned implicit function for high-resolution clothed human digitization. In *ICCV*, pages 2304–2314, 2019.
- [8] Shunsuke Saito, Tomas Simon, Jason Saragih, and Hanbyul Joo. PIFuHD: Multi-Level Pixel-Aligned Implicit Function for High-Resolution 3D Human Digitization. In *CVPR*, pages 81–90, 2020.
- [9] Thiemo Alldieck, Mihai Zanfir, and Cristian Sminchisescu. Photorealistic monocular 3d reconstruction of humans wearing clothing. In *Proceedings of the IEEE/CVF Conference on Computer Vision and Pattern Recognition*, pages 1506–1515, 2022.
- [10] Shoukang Hu, Fangzhou Hong, Liang Pan, Haiyi Mei, Lei Yang, and Ziwei Liu. Sherf: Generalizable human nerf from a single image. In *Proceedings of the IEEE/CVF International Conference on Computer Vision*, pages 9352–9364, 2023.
- [11] Yangyi Huang, Hongwei Yi, Weiyang Liu, Haofan Wang, Boxi Wu, Wenxiao Wang, Binbin Lin, Debing Zhang, and Deng Cai. One-shot implicit animatable avatars with model-based priors. In *IEEE Conference on Computer Vision (ICCV)*, 2023.
- [12] Jeong Joon Park, Peter Florence, Julian Straub, Richard Newcombe, and Steven Lovegrove. DeepSDF: Learning continuous signed distance functions for shape representation. In *Proceedings of the IEEE/CVF conference on computer vision and pattern recognition*, pages 165–174, 2019.
- [13] Ben Mildenhall, Pratul P Srinivasan, Matthew Tancik, Jonathan T Barron, Ravi Ramamoorthi, and Ren Ng. Nerf: Representing scenes as neural radiance fields for view synthesis. *Communications of the ACM*, 65(1):99–106, 2021.
- [14] Bernhard Kerbl, Georgios Kopanas, Thomas Leimkuehler, and George Drettakis. 3d gaussian splatting for real-time radiance field rendering. *ACM Transactions on Graphics (TOG)*, 42(4):1–14, 2023.
- [15] Wojciech Zielonka, Timur Bagautdinov, Shunsuke Saito, Michael Zollhöfer, Justus Thies, and Javier Romero. Drivable 3d gaussian avatars. *arXiv preprint arXiv:2311.08581*, 2023.
- [16] Arthur Moreau, Jifei Song, Helisa Dharmo, Richard Shaw, Yiren Zhou, and Eduardo Pérez-Pellitero. Human gaussian splatting: Real-time rendering of animatable avatars. *arXiv preprint arXiv:2311.17113*, 2023.
- [17] Zhiyin Qian, Shaofei Wang, Marko Mihajlovic, Andreas Geiger, and Siyu Tang. 3dgs-avatar: Animatable avatars via deformable 3d gaussian splatting. *arXiv preprint arXiv:2312.09228*, 2023.

- [18] Mengtian Li, Shengxiang Yao, Zhifeng Xie, Keyu Chen, and Yu-Gang Jiang. Gaussianbody: Clothed human reconstruction via 3d gaussian splatting. *arXiv preprint arXiv:2401.09720*, 2024.
- [19] Shoukang Hu and Ziwei Liu. Gauhuman: Articulated gaussian splatting from monocular human videos. *arXiv preprint arXiv:2312.02973*, 2023.
- [20] Liangxiao Hu, Hongwen Zhang, Yuxiang Zhang, Boyao Zhou, Boning Liu, Shengping Zhang, and Liqiang Nie. Gaussianavatar: Towards realistic human avatar modeling from a single video via animatable 3d gaussians. In *Proceedings of the IEEE/CVF Conference on Computer Vision and Pattern Recognition (CVPR)*, 2024.
- [21] Yangyi Huang, Hongwei Yi, Yuliang Xiu, Tingting Liao, Jiayang Tang, Deng Cai, and Justus Thies. TeCH: Text-guided Reconstruction of Lifelike Clothed Humans. In *International Conference on 3D Vision (3DV)*, 2024.
- [22] Badour AlBahar, Shunsuke Saito, Hung-Yu Tseng, Changil Kim, Johannes Kopf, and Jia-Bin Huang. Single-image 3d human digitization with shape-guided diffusion. In *SIGGRAPH Asia 2023 Conference Papers*, pages 1–11, 2023.
- [23] Xin Huang, Ruizhi Shao, Qi Zhang, Hongwen Zhang, Ying Feng, Yebin Liu, and Qing Wang. Humannorm: Learning normal diffusion model for high-quality and realistic 3d human generation. *arXiv preprint arXiv:2310.01406*, 2023.
- [24] Xihe Yang, Xingyu Chen, Shaohui Wang, Daiheng Gao, Xiaoguang Han, and Baoyuan Wang. Have-fun: Human avatar reconstruction from few-shot unconstrained images. *arXiv preprint arXiv:2311.15672*, 2023.
- [25] Ben Poole, Ajay Jain, Jonathan T Barron, and Ben Mildenhall. Dreamfusion: Text-to-3d using 2d diffusion. In *International Conference on Learning Representations (ICLR)*, 2023.
- [26] Jiteng Mu, Shen Sang, Nuno Vasconcelos, and Xiaolong Wang. Actorsnerf: Animatable few-shot human rendering with generalizable nerfs. In *Proceedings of the IEEE/CVF International Conference on Computer Vision*, pages 18391–18401, 2023.
- [27] Zhenzhen Weng, Jingyuan Liu, Hao Tan, Zhan Xu, Yang Zhou, Serena Yeung-Levy, and Jimei Yang. Template-free single-view 3d human digitalization with diffusion-guided lrm, 2024.
- [28] Shunyuan Zheng, Boyao Zhou, Ruizhi Shao, Boning Liu, Shengping Zhang, Liqiang Nie, and Yebin Liu. Gps-gaussian: Generalizable pixel-wise 3d gaussian splatting for real-time human novel view synthesis. *arXiv preprint arXiv:2312.02155*, 2023.
- [29] Jiayang Tang, Zhaoxi Chen, Xiaokang Chen, Tengfei Wang, Gang Zeng, and Ziwei Liu. Lgm: Large multi-view gaussian model for high-resolution 3d content creation. *arXiv preprint arXiv:2402.05054*, 2024.
- [30] Zechuan Zhang, Li Sun, Zongxin Yang, Ling Chen, and Yi Yang. Global-correlated 3d-decoupling transformer for clothed avatar reconstruction. *Advances in Neural Information Processing Systems*, 36, 2024.
- [31] Angjoo Kanazawa, Michael J. Black, David W. Jacobs, and Jitendra Malik. End-to-end recovery of human shape and pose. In *CVPR*, pages 7122–7131, 2018.
- [32] Muhammed Kocabas, Chun-Hao P. Huang, Otmar Hilliges, and Michael J. Black. PARE: Part attention regressor for 3D human body estimation. In *ICCV*, pages 11127–11137, 2021.
- [33] Hongwen Zhang, Yating Tian, Yuxiang Zhang, Mengcheng Li, Liang An, Zhenan Sun, and Yebin Liu. PyMAF-X: Towards Well-aligned Full-body Model Regression from Monocular Images. *IEEE TPAMI*, 2023.
- [34] Jiefeng Li, Siyuan Bian, Qi Liu, Jiasheng Tang, Fan Wang, and Cewu Lu. NIKI: Neural inverse kinematics with invertible neural networks for 3d human pose and shape estimation. In *CVPR*, June 2023.
- [35] Xin Chen, Zhuo Su, Lingbo Yang, Pei Cheng, Lan Xu, Bin Fu, and Gang Yu. Learning variational motion prior for video-based motion capture. *arXiv preprint arXiv:2210.15134*, 2022.
- [36] Muhammed Kocabas, Nikos Athanasiou, and Michael J. Black. VIBE: Video inference for human body pose and shape estimation. In *CVPR*, pages 5252–5262, 2020.

- [37] Nikos Kolotouros, Georgios Pavlakos, Michael J. Black, and Kostas Daniilidis. Learning to reconstruct 3D human pose and shape via model-fitting in the loop. In *ICCV*, pages 2252–2261, 2019.
- [38] Thiemo Alldieck, Marcus A. Magnor, Weipeng Xu, Christian Theobalt, and Gerard Pons-Moll. Video based reconstruction of 3D people models. In *CVPR*, 2018.
- [39] Thiemo Alldieck, Marcus A. Magnor, Bharat Lal Bhatnagar, Christian Theobalt, and Gerard Pons-Moll. Learning to reconstruct people in clothing from a single RGB camera. In *CVPR*, 2019.
- [40] Hao Zhu, Xinxin Zuo, Sen Wang, Xun Cao, and Ruigang Yang. Detailed human shape estimation from a single image by hierarchical mesh deformation. In *CVPR*, 2019.
- [41] Verica Lazova, Eldar Insafutdinov, and Gerard Pons-Moll. 360-Degree textures of people in clothing from a single image. In *International Conference on 3D Vision (3DV)*, 2019.
- [42] Bharat Lal Bhatnagar, Garvita Tiwari, Christian Theobalt, and Gerard Pons-Moll. Multi-Garment Net: Learning to dress 3D people from images. In *ICCV*, 2019.
- [43] Boyi Jiang, Juyong Zhang, Yang Hong, Jinhao Luo, Ligang Liu, and Hujun Bao. BCNet: Learning body and cloth shape from a single image. In *ECCV*, 2020.
- [44] Yao Feng, Weiyang Liu, Timo Bolkart, Jinlong Yang, Marc Pollefeys, and Michael J. Black. Learning disentangled avatars with hybrid 3d representations, 2023.
- [45] Sang-Hun Han, Min-Gyu Park, Ju Hong Yoon, Ju-Mi Kang, Young-Jae Park, and Hae-Gon Jeon. High-fidelity 3d human digitization from single 2k resolution images. In *Proceedings of the IEEE/CVF Conference on Computer Vision and Pattern Recognition (CVPR)*, 2023.
- [46] Badour AlBahar, Shunsuke Saito, Hung-Yu Tseng, Changil Kim, Johannes Kopf, and Jia-Bin Huang. Single-image 3d human digitization with shape-guided diffusion. In *SIGGRAPH Asia*, 2023.
- [47] Muxin Zhang, Qiao Feng, Zhuo Su, Chao Wen, Zhou Xue, and Kun Li. Joint2human: High-quality 3d human generation via compact spherical embedding of 3d joints. In *Proceedings of the IEEE/CVF Conference on Computer Vision and Pattern Recognition (CVPR)*, pages 1429–1438, June 2024.
- [48] Tong He, John P. Collomosse, Hailin Jin, and Stefano Soatto. Geo-PIFu: Geometry and pixel aligned implicit functions for single-view human reconstruction. In *NeurIPS*, 2020.
- [49] Enric Corona, Mihai Zanfir, Thiemo Alldieck, Eduard Gabriel Bazavan, Andrei Zanfir, and Cristian Sminchisescu. Structured 3d features for reconstructing relightable and animatable avatars. In *CVPR*, 2023.
- [50] Yuliang Xiu, Jinlong Yang, Dimitrios Tzionas, and Michael J. Black. ICON: Implicit Clothed humans Obtained from Normals. In *CVPR*, 2022.
- [51] Zerong Zheng, Tao Yu, Yebin Liu, and Qionghai Dai. PaMIR: Parametric Model-conditioned Implicit Representation for image-based human reconstruction. *IEEE TPAMI*, 44(6):3170–3184, 2021.
- [52] Zeng Huang, Yuanlu Xu, Christoph Lassner, Hao Li, and Tony Tung. ARCH: Animatable Reconstruction of Clothed Humans. In *CVPR*, pages 3093–3102, 2020.
- [53] Tong He, Yuanlu Xu, Shunsuke Saito, Stefano Soatto, and Tony Tung. ARCH++: Animation-Ready Clothed Human Reconstruction Revisited. In *ICCV*, pages 11046–11056, 2021.
- [54] Yukang Cao, Guanying Chen, Kai Han, Wenqi Yang, and Kwan-Yee K. Wong. JIFF: Jointly-aligned Implicit Face Function for High Quality Single View Clothed Human Reconstruction. In *CVPR*, 2022.
- [55] Tingting Liao, Xiaomei Zhang, Yuliang Xiu, Hongwei Yi, Xudong Liu, Guo-Jun Qi, Yong Zhang, Xuan Wang, Xiangyu Zhu, and Zhen Lei. High-Fidelity Clothed Avatar Reconstruction from a Single Image. In *CVPR*, June 2023.
- [56] Xueting Yang, Yihao Luo, Yuliang Xiu, Wei Wang, Hao Xu, and Zhaoxin Fan. D-if: Uncertainty-aware human digitization via implicit distribution field. In *Proceedings of the IEEE/CVF International Conference on Computer Vision*, pages 9122–9132, 2023.

- [57] Yukang Cao, Kai Han, and Kwan-Yee K. Wong. Sesdf: Self-evolved signed distance field for implicit 3d clothed human reconstruction. In *IEEE Conference on Computer Vision and Pattern Recognition (CVPR)*, 2023.
- [58] Zechuan Zhang, Li Sun, Zongxin Yang, Ling Chen, and Yi Yang. Global-correlated 3d-decoupling transformer for clothed avatar reconstruction. In *Advances in Neural Information Processing Systems (NeurIPS)*, 2023.
- [59] Zhuo Su, Lan Xu, Zerong Zheng, Tao Yu, Yebin Liu, and Lu Fang. Robustfusion: Human volumetric capture with data-driven visual cues using a rgbd camera. In Andrea Vedaldi, Horst Bischof, Thomas Brox, and Jan-Michael Frahm, editors, *Computer Vision – ECCV 2020*, pages 246–264, Cham, 2020. Springer International Publishing.
- [60] Zhuo Su, Lan Xu, Dawei Zhong, Zhong Li, Fan Deng, Shuxue Quan, and Lu Fang. Robustfusion: Robust volumetric performance reconstruction under human-object interactions from monocular rgbd stream. *IEEE Transactions on Pattern Analysis and Machine Intelligence*, 2022.
- [61] Yuliang Xiu, Jinlong Yang, Xu Cao, Dimitrios Tzionas, and Michael J. Black. ECON: Explicit Clothed humans Optimized via Normal integration. In *CVPR*, June 2023.
- [62] Yuheng Jiang, Kaixin Yao, Zhuo Su, Zhehao Shen, Haimin Luo, and Lan Xu. Instant-nvr: Instant neural volumetric rendering for human-object interactions from monocular rgbd stream. In *Proceedings of the IEEE/CVF Conference on Computer Vision and Pattern Recognition (CVPR)*, pages 595–605, June 2023.
- [63] Xiaozheng Zheng, Chao Wen, Zhuo Su, Zeran Xu, Zhaohu Li, Yang Zhao, and Zhou Xue. Ohta: One-shot hand avatar via data-driven implicit priors, 2024.
- [64] Yangyi Huang, Hongwei Yi, Yuliang Xiu, Tingting Liao, Jiayang Tang, Deng Cai, and Justus Thies. TeCH: Text-guided Reconstruction of Lifelike Clothed Humans. In *International Conference on 3D Vision (3DV)*, 2024.
- [65] Alec Radford, Jong Wook Kim, Chris Hallacy, Aditya Ramesh, Gabriel Goh, Sandhini Agarwal, Girish Sastry, Amanda Askell, Pamela Mishkin, Jack Clark, et al. Learning transferable visual models from natural language supervision. In *International conference on machine learning*, pages 8748–8763. PMLR, 2021.
- [66] Bernhard Kerbl, Georgios Kopanas, Thomas Leimkühler, and George Drettakis. 3d gaussian splatting for real-time radiance field rendering. *ACM Transactions on Graphics*, 42(4), July 2023.
- [67] Yuheng Jiang, Zhehao Shen, Penghao Wang, Zhuo Su, Yu Hong, Yingliang Zhang, Jingyi Yu, and Lan Xu. Hifi4g: High-fidelity human performance rendering via compact gaussian splatting. In *Proceedings of the IEEE/CVF Conference on Computer Vision and Pattern Recognition (CVPR)*, 2024.
- [68] Haokai Pang, Heming Zhu, Adam Kortylewski, Christian Theobalt, and Marc Habermann. Ash: Animatable gaussian splats for efficient and photoreal human rendering. 2024.
- [69] Zhe Li, Zerong Zheng, Lizhen Wang, and Yebin Liu. Animatable gaussians: Learning pose-dependent gaussian maps for high-fidelity human avatar modeling. In *CVPR*, 2024.
- [70] Mingwei Li, Jiachen Tao, Zongxin Yang, and Yi Yang. Human101: Training 100+ fps human gaussians in 100s from 1 view. *arXiv preprint arXiv:2312.15258*, 2023.
- [71] Xinqi Liu, Chenming Wu, Jialun Liu, Xing Liu, Chen Zhao, Haocheng Feng, Errui Ding, and Jingdong Wang. Gva: Reconstructing vivid 3d gaussian avatars from monocular videos. *Arxiv*, 2024.
- [72] Zhijing Shao, Zhaolong Wang, Zhuang Li, Duotun Wang, Xiangru Lin, Yu Zhang, Mingming Fan, and Zeyu Wang. SplattingAvatar: Realistic Real-Time Human Avatars with Mesh-Embedded Gaussian Splatting. In *CVPR*, 2024.
- [73] Jing Wen, Xiaoming Zhao, Zhongzheng Ren, Alexander G. Schwing, and Shenlong Wang. Gomavatar: Efficient animatable human modeling from monocular video using gaussians-on-mesh, 2024.
- [74] Jiahui Lei, Yufu Wang, Georgios Pavlakos, Lingjie Liu, and Kostas Daniilidis. Gart: Gaussian articulated template models. In *Proceedings of the IEEE/CVF Conference on Computer Vision and Pattern Recognition (CVPR)*, 2024.

- [75] David Svitov, Pietro Morerio, Lourdes Agapito, and Alessio Del Bue. Haha: Highly articulated gaussian human avatars with textured mesh prior. *arXiv preprint arXiv:2404.01053*, 2024.
- [76] Yicong Hong, Kai Zhang, Jiuxiang Gu, Sai Bi, Yang Zhou, Difan Liu, Feng Liu, Kalyan Sunkavalli, Trung Bui, and Hao Tan. Lrm: Large reconstruction model for single image to 3d. *arXiv preprint arXiv:2311.04400*, 2023.
- [77] Dmitry Tochilkin, David Pankratz, Zexiang Liu, Zixuan Huang, Adam Letts, Yangguang Li, Ding Liang, Christian Laforte, Varun Jampani, and Yan-Pei Cao. Triposr: Fast 3d object reconstruction from a single image. *arXiv preprint arXiv:2403.02151*, 2024.
- [78] Ashish Vaswani, Noam Shazeer, Niki Parmar, Jakob Uszkoreit, Llion Jones, Aidan N Gomez, Łukasz Kaiser, and Illia Polosukhin. Attention is all you need. *Advances in Neural Information Processing Systems (NeurIPS)*, 30, 2017.
- [79] Zi-Xin Zou, Zhipeng Yu, Yuan-Chen Guo, Yangguang Li, Ding Liang, Yan-Pei Cao, and Song-Hai Zhang. Triplane meets gaussian splatting: Fast and generalizable single-view 3d reconstruction with transformers. In *Proceedings of the IEEE/CVF Conference on Computer Vision and Pattern Recognition (CVPR)*, 2023.
- [80] Yichun Shi, Peng Wang, Jianglong Ye, Long Mai, Kejie Li, and Xiao Yang. Mvdream: Multi-view diffusion for 3d generation. In *International Conference on Learning Representations (ICLR)*, 2024.
- [81] Peng Wang and Yichun Shi. Imagedream: Image-prompt multi-view diffusion for 3d generation. *arXiv preprint arXiv:2312.02201*, 2023.
- [82] Ruoxi Shi, Hansheng Chen, Zhuoyang Zhang, Minghua Liu, Chao Xu, Xinyue Wei, Linghao Chen, Chong Zeng, and Hao Su. Zero123++: a single image to consistent multi-view diffusion base model. *arXiv preprint arXiv:2310.15110*, 2023.
- [83] Jiahao Li, Hao Tan, Kai Zhang, Zexiang Xu, Fujun Luan, Yinghao Xu, Yicong Hong, Kalyan Sunkavalli, Greg Shakhnarovich, and Sai Bi. Instant3d: Fast text-to-3d with sparse-view generation and large reconstruction model. *arXiv preprint arXiv:2311.06214*, 2023.
- [84] Zhengyi Wang, Yikai Wang, Yifei Chen, Chendong Xiang, Shuo Chen, Dajiang Yu, Chongxuan Li, Hang Su, and Jun Zhu. Crm: Single image to 3d textured mesh with convolutional reconstruction model. *arXiv preprint arXiv:2403.05034*, 2024.
- [85] Xinyue Wei, Kai Zhang, Sai Bi, Hao Tan, Fujun Luan, Valentin Deschaintre, Kalyan Sunkavalli, Hao Su, and Zexiang Xu. Meshlrm: Large reconstruction model for high-quality mesh. *arXiv preprint arXiv:2404.12385*, 2024.
- [86] Jiale Xu, Weihao Cheng, Yiming Gao, Xintao Wang, Shenghua Gao, and Ying Shan. Instantmesh: Efficient 3d mesh generation from a single image with sparse-view large reconstruction models. *arXiv preprint arXiv:2404.07191*, 2024.
- [87] Tianchang Shen, Jacob Munkberg, Jon Hasselgren, Kangxue Yin, Zian Wang, Wenzheng Chen, Zan Gojcic, Sanja Fidler, Nicholas Sharp, and Jun Gao. Flexible isosurface extraction for gradient-based mesh optimization. *ACM Transactions on Graphics (TOG)*, 42(4):1–16, 2023.
- [88] Jiaxiang Tang, Zhaoxi Chen, Xiaokang Chen, Tengfei Wang, Gang Zeng, and Ziwei Liu. Lgm: Large multi-view gaussian model for high-resolution 3d content creation. *arXiv preprint arXiv:2402.05054*, 2024.
- [89] Yinghao Xu, Zifan Shi, Wang Yifan, Hansheng Chen, Ceyuan Yang, Sida Peng, Yujun Shen, and Gordon Wetzstein. Grm: Large gaussian reconstruction model for efficient 3d reconstruction and generation. *arXiv preprint arXiv:2403.14621*, 2024.
- [90] Kai Zhang, Sai Bi, Hao Tan, Yuanbo Xiangli, Nanxuan Zhao, Kalyan Sunkavalli, and Zexiang Xu. Gs-lrm: Large reconstruction model for 3d gaussian splatting. *arXiv preprint arXiv:2404.19702*, 2024.
- [91] Stanislaw Szymanowicz, Christian Rupprecht, and Andrea Vedaldi. Splatter image: Ultra-fast single-view 3d reconstruction. In *Proceedings of the IEEE/CVF Conference on Computer Vision and Pattern Recognition (CVPR)*, 2024.
- [92] David Charatan, Sizhe Li, Andrea Tagliasacchi, and Vincent Sitzmann. pixelsplat: 3d gaussian splats from image pairs for scalable generalizable 3d reconstruction. In *Proceedings of the IEEE/CVF Conference on Computer Vision and Pattern Recognition (CVPR)*, 2024.

- [93] Hao-Yang Peng, Jia-Peng Zhang, Meng-Hao Guo, Yan-Pei Cao, and Shi-Min Hu. Charactergen: Efficient 3d character generation from single images with multi-view pose canonicalization. *arXiv preprint arXiv:2402.17214*, 2024.
- [94] Yao Feng, Vasileios Choutas, Timo Bolkart, Dimitrios Tzionas, and Michael J Black. Collaborative regression of expressive bodies using moderation. In *2021 International Conference on 3D Vision (3DV)*, pages 792–804. IEEE, 2021.
- [95] Georgios Pavlakos, Vasileios Choutas, Nima Ghorbani, Timo Bolkart, Ahmed A. A. Osman, Dimitrios Tzionas, and Michael J. Black. Expressive body capture: 3D hands, face, and body from a single image. In *CVPR*, pages 10975–10985, 2019.
- [96] Vikram Voleti, Chun-Han Yao, Mark Boss, Adam Letts, David Pankratz, Dmitry Tochilkin, Christian Laforte, Robin Rombach, and Varun Jampani. Sv3d: Novel multi-view synthesis and 3d generation from a single image using latent video diffusion. *arXiv preprint arXiv:2403.12008*, 2024.
- [97] Patrick Esser, Robin Rombach, and Bjorn Ommer. Taming transformers for high-resolution image synthesis. In *Proceedings of the IEEE/CVF conference on computer vision and pattern recognition*, pages 12873–12883, 2021.
- [98] Andreas Blattmann, Tim Dockhorn, Sumith Kulal, Daniel Mendelevitch, Maciej Kilian, Dominik Lorenz, Yam Levi, Zion English, Vikram Voleti, Adam Letts, et al. Stable video diffusion: Scaling latent video diffusion models to large datasets. *arXiv preprint arXiv:2311.15127*, 2023.
- [99] Matt Deitke, Dustin Schwenk, Jordi Salvador, Luca Weihs, Oscar Michel, Eli VanderBilt, Ludwig Schmidt, Kiana Ehsani, Aniruddha Kembhavi, and Ali Farhadi. Objaverse: A universe of annotated 3d objects. In *Proceedings of the IEEE/CVF Conference on Computer Vision and Pattern Recognition (CVPR)*, pages 13142–13153, 2023.
- [100] Yinghao Xu, Hao Tan, Fujun Luan, Sai Bi, Peng Wang, Jiahao Li, Zifan Shi, Kalyan Sunkavalli, Gordon Wetzstein, Zexiang Xu, et al. Dmv3d: Denoising multi-view diffusion using 3d large reconstruction model. *arXiv preprint arXiv:2311.09217*, 2023.
- [101] Eric Ming Chen, Sidhanth Holalkere, Ruyi Yan, Kai Zhang, and Abe Davis. Ray conditioning: Trading photo-consistency for photo-realism in multi-view image generation. In *Proceedings of the IEEE/CVF International Conference on Computer Vision (ICCV)*, pages 23242–23251, October 2023.
- [102] Julius Plücker. Xvii. on a new geometry of space. *Philosophical Transactions of the Royal Society of London*, (155):725–791, 1865.
- [103] Alexey Dosovitskiy, Lucas Beyer, Alexander Kolesnikov, Dirk Weissenborn, Xiaohua Zhai, Thomas Unterthiner, Mostafa Dehghani, Matthias Minderer, Georg Heigold, Sylvain Gelly, et al. An image is worth 16x16 words: Transformers for image recognition at scale. In *International Conference on Learning Representations*, 2020.
- [104] Thiemo Alldieck, Marcus Magnor, Bharat Lal Bhatnagar, Christian Theobalt, and Gerard Pons-Moll. Learning to reconstruct people in clothing from a single rgb camera. In *Proceedings of the IEEE/CVF Conference on Computer Vision and Pattern Recognition*, pages 1175–1186, 2019.
- [105] Zechuan Zhang, Zongxin Yang, and Yi Yang. Sifu: Side-view conditioned implicit function for real-world usable clothed human reconstruction. *arXiv preprint arXiv:2312.06704*, 2023.
- [106] Richard Zhang, Phillip Isola, Alexei A Efros, Eli Shechtman, and Oliver Wang. The unreasonable effectiveness of deep features as a perceptual metric. In *Proceedings of the IEEE conference on computer vision and pattern recognition*, pages 586–595, 2018.
- [107] Tao Yu, Zerong Zheng, Kaiwen Guo, Pengpeng Liu, Qionghai Dai, and Yebin Liu. Function4d: Real-time human volumetric capture from very sparse consumer rgbd sensors. In *IEEE Conference on Computer Vision and Pattern Recognition (CVPR2021)*, June 2021.
- [108] Sang-Hun Han, Min-Gyu Park, Ju Hong Yoon, Ju-Mi Kang, Young-Jae Park, and Hae-Gon Jeon. High-fidelity 3d human digitization from single 2k resolution images. In *Proceedings of the IEEE/CVF Conference on Computer Vision and Pattern Recognition*, pages 12869–12879, 2023.
- [109] Twindom. <https://web.twindom.com/>.

- [110] Zhou Wang, Alan C Bovik, Hamid R Sheikh, and Eero P Simoncelli. Image quality assessment: from error visibility to structural similarity. *IEEE transactions on image processing*, 13(4):600–612, 2004.
- [111] Ben Poole, Ajay Jain, Jonathan T Barron, and Ben Mildenhall. Dreamfusion: Text-to-3d using 2d diffusion. In *International Conference on Learning Representations (ICLR)*, 2023.
- [112] Haochen Wang, Xiaodan Du, Jiahao Li, Raymond A Yeh, and Greg Shakhnarovich. Score jacobian chaining: Lifting pretrained 2d diffusion models for 3d generation. In *Proceedings of the IEEE/CVF Conference on Computer Vision and Pattern Recognition*, pages 12619–12629, 2023.
- [113] Shunsuke Saito, Zeng Huang, Ryota Natsume, Shigeo Morishima, Angjoo Kanazawa, and Hao Li. Pifu: Pixel-aligned implicit function for high-resolution clothed human digitization. In *The IEEE International Conference on Computer Vision (ICCV)*, October 2019.
- [114] Zhongcong Xu, Jianfeng Zhang, Jun Hao Liew, Hanshu Yan, Jia-Wei Liu, Chenxu Zhang, Jiashi Feng, and Mike Zheng Shou. Magicanimate: Temporally consistent human image animation using diffusion model. *arXiv preprint arXiv:2311.16498*, 2023.
- [115] Robin Rombach, Andreas Blattmann, Dominik Lorenz, Patrick Esser, and Björn Ommer. High-resolution image synthesis with latent diffusion models. In *Proceedings of the IEEE/CVF Conference on Computer Vision and Pattern Recognition (CVPR)*, pages 10684–10695, 2022.
- [116] Yang Song, Jascha Sohl-Dickstein, Diederik P Kingma, Abhishek Kumar, Stefano Ermon, and Ben Poole. Score-based generative modeling through stochastic differential equations. In *International Conference on Learning Representations (ICLR)*, 2021.
- [117] Tero Karras, Miika Aittala, Timo Aila, and Samuli Laine. Elucidating the design space of diffusion-based generative models. *Advances in Neural Information Processing Systems (NeurIPS)*, 35:26565–26577, 2022.
- [118] Jonathan Ho and Tim Salimans. Classifier-free diffusion guidance. In *NeurIPS 2021 Workshop on Deep Generative Models and Downstream Applications*, 2021.
- [119] Qi Zuo, Xiaodong Gu, Lingteng Qiu, Yuan Dong, Zhengyi Zhao, Weihao Yuan, Rui Peng, Siyu Zhu, Zilong Dong, Liefeng Bo, et al. Videomv: Consistent multi-view generation based on large video generative model. *arXiv preprint arXiv:2403.12010*, 2024.
- [120] Ilya Loshchilov and Frank Hutter. Decoupled weight decay regularization. *arXiv preprint arXiv:1711.05101*, 2017.
- [121] Tri Dao. Flashattention-2: Faster attention with better parallelism and work partitioning. *arXiv preprint arXiv:2307.08691*, 2023.
- [122] Benjamin Lefaudeux, Francisco Massa, Diana Liskovich, Wenhan Xiong, Vittorio Caggiano, Sean Naren, Min Xu, Jieru Hu, Marta Tintore, Susan Zhang, Patrick Labatut, Daniel Haziza, Luca Wehrstedt, Jeremy Reizenstein, and Grigory Sizov. xformers: A modular and hackable transformer modelling library. <https://github.com/facebookresearch/xformers>, 2022.
- [123] Tianqi Chen, Bing Xu, Chiyuan Zhang, and Carlos Guestrin. Training deep nets with sublinear memory cost. *arXiv preprint arXiv:1604.06174*, 2016.
- [124] Paulius Micikevicius, Sharan Narang, Jonah Alben, Gregory Diamos, Erich Elsen, David Garcia, Boris Ginsburg, Michael Houston, Oleksii Kuchaiev, Ganesh Venkatesh, et al. Mixed precision training. In *International Conference on Learning Representations*, 2018.
- [125] Li Hu, Xin Gao, Peng Zhang, Ke Sun, Bang Zhang, and Liefeng Bo. Animate anyone: Consistent and controllable image-to-video synthesis for character animation. *arXiv preprint arXiv:2311.17117*, 2023.

A Implementation Details

A.1 Additional novel View Synthesizer Details

The conditions of Diffusion model. SVD and SV3D [96, 98] replace CLIP text embeddings [65] with the image embedding of the conditioning. Compared to text prompts, image prompts provide information more accurately and directly, and also save time that would otherwise be spent on text inversion or image caption [21, 105].

Transformer Block. The CLIP embedding matrix from the conditioning image is fed into the cross-attention layers of each transformer block, acting as the key and value, while the feature at that layer serves as the query. Moreover, the camera trajectory and the diffusion noise timestep are incorporated into the residual blocks.

Fine-tuning details. We involve utilizing the widely used EDM [116, 117] framework, incorporating a simplified diffusion loss for finetuning. Finetuning at 512-res uses 1000-step warmup with the peak learning rate $1e-4$ in the cosine learning rate decay schedule. We use a per-GPU batch size of 8 objects/scenes during 256-res training, and a per-GPU batch size of 2 during 512-res finetuning. For each object, we use 4 input views and 4 novel supervision views at each iteration of 256-res and 512-res finetuning.

Triangular CFG Scaling. Classifier-free Guidance (CFG) [118] is a widely used technique to trade off controllability with diversity. However, this scaling causes the last few frames in our generated orbits to be over-sharpened. To tackle this issue, we use a triangle wave CFG [96, 119] scaling during inference: linearly increase CFG from 1 at the front view to 2.5 at the back view, then linearly decrease it back to 1.

A.2 Additional Latent Reconstruction Transformer Details

The network architecture of the proposed latent reconstruction transformer is shown in Fig. 6. The framework is composed of a latent encoder with intra- and inter-attention and a Gaussian parameter prediction module. It takes initial multi-view latent embeddings as input and performs projection-aware attention to aggregate human geometric information. From each output token, we decode the attributes of pixel-aligned Gaussians in the corresponding patch with a Conv 1×1 layer.

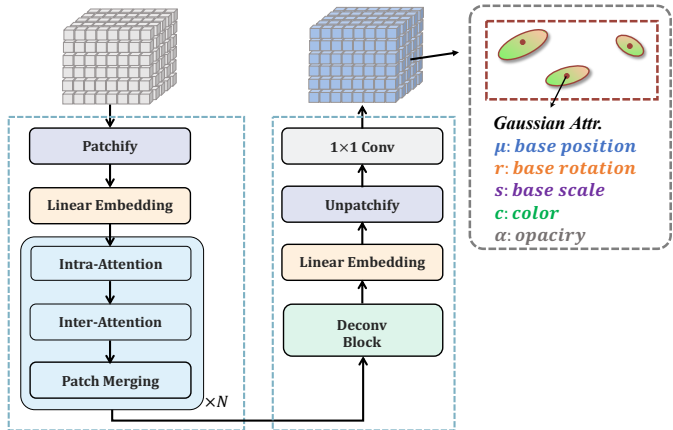


Figure 6: Detailed network architecture of latent reconstruction transformer.

A.3 Additional Training Details

We train our model with AdamW [120] optimizer. The β_1, β_2 are set to 0.9 and 0.95 respectively. We use a weight decay of 0.05 on all parameters except the those of the LayNorm layers. We use a cosine learning rate decay with linear warmup. We take 2000 step of warm up and the peak learning

rate is set to $4e-4$. For parts related to the head, hands, and arms, $\hat{\mathbf{I}}_{\text{part},j}$ is set to 2, while the rest are set to 1. The parameters λ_p and λ_m are set to 1. The model is trained for 80K iterations on the 256-res training, and then fine-tuned with 512-res for another 20K iterations. To enable efficient training and inference, we adopt Flash-Attention-v2 [121] in the xFormers [122] library, gradient checkpointing [123], and mixed-precision training [124] with FP16 data type. 256-res training takes about 2 days on 8 A100 (40G VRAM) GPUs, while 512-res finetuning costs 2 additional days.

Table 3: Evaluation of different window sizes K_{win} on the 2K2K evaluation dataset.

Method	PSNR \uparrow	SSIM \uparrow	LPIPS \downarrow
w/o Human Prior	22.635 (-1.658)	0.893 (-0.022)	0.182 (+0.142)
$K_{win} = 1$	23.333 (-0.960)	0.916 (-0.001)	0.057 (+0.017)
$K_{win} = 3$	24.383 (+0.089)	0.931 (+0.016)	0.041 (+0.001)
$K_{win} = 4$	24.013 (-0.280)	0.922 (+0.007)	0.048 (+0.008)
$K_{win} = 2$ (Ours)	24.293	0.915	0.040

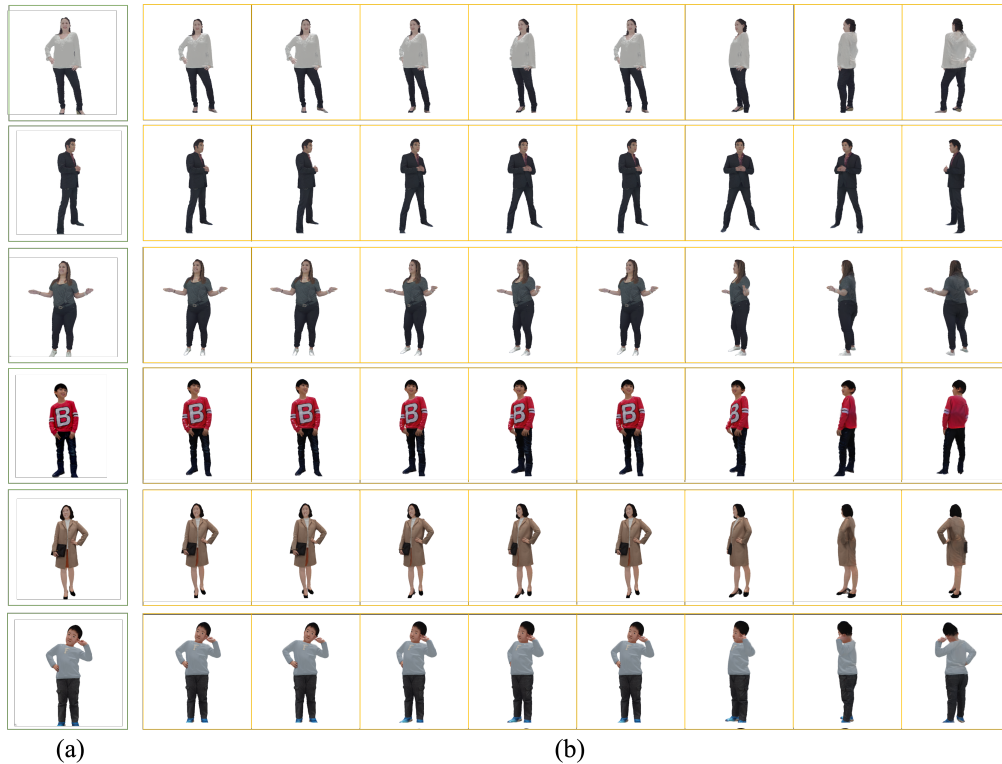


Figure 7: Qualitative 3D Gaussian Splatting results of diversified evaluation dataset. (a) Input Image. (b) Novel view Rendering Results.

B More Results.

In Tab. 3, we present results for the 2K2K dataset across various window sizes. The results show that employing a window size of $k_{win} = 1$ significantly enhances performance, improving the PSNR metric from 22.635 db to 23.333 db. Further refinement with a window size of $k_{win} = 3$ continues to enhance the results, whereas using $k_{win} = 4$ does not yield additional improvements. After considering both computational complexity and metrics, we selected a window size of $K_{win} = 2$.

As for novel view and novel pose rendering, more results are shown in Fig. 7 and Fig. 8. For a single input image, we use AnimateAnyone [125] for novel pose synthesis and HumanSplat for novel view synthesis. This functionality enables dynamic timestamps and real-time rendering of novel views,

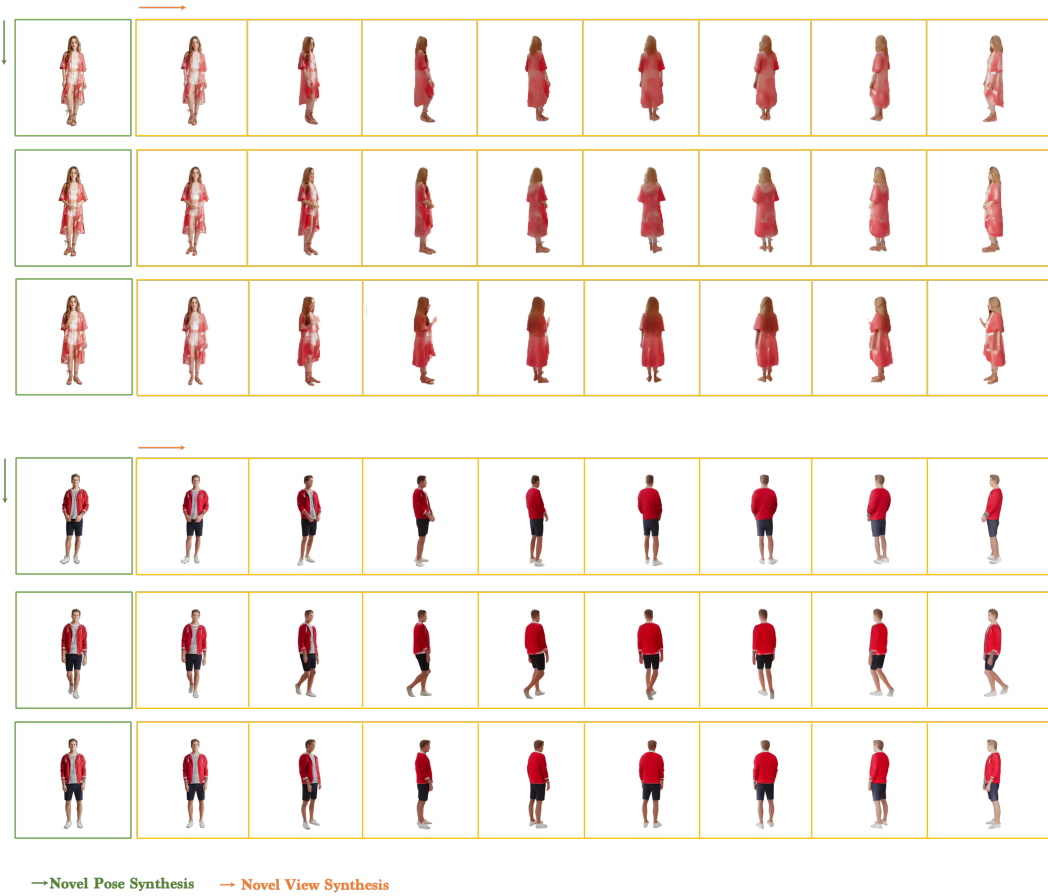


Figure 8: Qualitative 4D Gaussian Splatting results on In-the-wild images, including novel view and pose rendering results.

thereby enhancing immersive virtual exploration. Please also kindly refer to our supplementary video for more results.

C Broader Impacts

While our model demonstrates the capability to reconstruct photo-realistic 3D avatars, it also introduces potential risks such as privacy violations. To mitigate these concerns, it is imperative to establish robust ethical guidelines and legal frameworks. This necessitates a collaborative effort among researchers, developers, and policymakers to promote the responsible use of this technology and safeguard against its potential misuse.